Human Pathology (2019) **83**, 177–191

ELSEVIER

Human PATHOLOGY

www.elsevier.com/locate/humpath

Original contribution

Usefulness of complementary next-generation sequencing and quantitative immunohistochemistry panels for predicting brain metastases and selecting treatment outcomes of non–small cell lung cancer☆,☆☆

Juliana Machado-Rugolo PhD[a], Alexandre Todorovic Fabro MD, PhD[b], Daniel Ascheri MD[c], Cecília Farhat PhD[c], Alexandre Muxfeldt Ab'Saber MD, PhD[c], Vanessa Karen de Sá PhD[c], Maria Aparecida Nagai PhD[d], Teresa Takagaki MD, PhD[e], Ricardo Terra MD, PhD[f,g], Edwin Roger Parra MD, PhD[h], Vera Luiza Capelozzi MD, PhD[c,*]

[a]*Clinicas Hospital, Faculty of Medicine, State University of São Paulo, Botucatu 18618-682, Brazil*
[b]*Department of Pathology and Legal Medicine, Ribeirão Preto School of Medicine, University of São Paulo, Ribeirão Preto 14049-900, Brazil*
[c]*Laboratory of Genomics and Histomorphometry, Department of Pathology, University of São Paulo Medical School, São Paulo 01246-903, Brazil*
[d]*Department of Oncology, Clinicas Hospital, São Paulo 01246-903, Brazil*
[e]*Division of Pneumology, Heart Institute (Incor), Faculty of Medicine, University of São Paulo, São Paulo 01246-903, Brazil*
[f]*Department of Thoracic Surgery, Institute of Cancer of São Paulo, São Paulo 01246-903, Brazil*
[g]*Department of Thoracic Surgery, Heart Institute (Incor), São Paulo 01246-903, Brazil*
[h]*Department of Translational Molecular Pathology, The University of Texas MD Anderson Cancer Center, Houston, TX 77030, USA*

Received 29 June 2018; revised 24 August 2018; accepted 29 August 2018

Keywords:
Epithelial-mesenchymal transition;
Immunohistochemistry;
Next-generation sequencing;
H-score;
Adenocarcinoma;
Squamouscell carcinoma;
Large cell carcinoma

Summary To demonstrate the usefulness of complementary next-generation sequencing (NGS) and immunohistochemistry (IHC) counting, we analyzed 196 patients with non–small cell lung cancer who underwent surgical resection and adjuvant chemotherapy. Formalin-fixed, paraffin-embedded samples of adenocarcinoma (ADC), squamous cell carcinoma, and large cell carcinoma were used to prepare tissue microarrays and were examined by protein H-score IHC image analysis and NGS for oncogenes and proto-oncogenes and genes of tumor suppressors, immune checkpoints, epithelial-mesenchymal transition factors, tyrosine kinase receptors, and vascular endothelial growth factors. In patients with brain metastases, primary tumors expressed lower PIK3CA protein levels. Overexpression of p53 and a higher PD-L1 protein H-score were detected in patients who underwent surgical treatment followed by chemotherapy as compared with those

☆ Competing interest: The authors declare that they have no conflicts of interest.

☆☆ Funding/Support: The University of Texas Lung Specialized Programs of Research Excellence grant (P50CA70907) and MD Anderson's Cancer Center Support Grant (2P30CA016672; used the Tissue Biospecimen and Pathology Resource) from the National Cancer Institute; National Counsel of Technological and Scientific Development of the Ministry of Science-CNPq, Technology and Innovation of Brazil (P246042/2012-5); and the Foundation for the Support of Research of the State of São Paulo (FAPESP 2013/14277-4).

* Corresponding author at: Department of Pathology, Faculdade de Medicina da Universidade de São Paulo, Av Dr Arnaldo 455, Room 1143, São Paulo, 01246-903, SP, Brazil.
E-mail address: vera.capelozzi@fm.usp.br (V. L. Capelozzi).

https://doi.org/10.1016/j.humpath.2018.08.026

who underwent only surgical treatment The absence of brain metastases was associated with wild-type sequences of genes *EGFR*, *CD267*, *CTLA-4*, and *ZEB1*. The combination of protein overexpression according to IHC and mutation according to NGS was rare (ie, represented by a very low percentage of concordant cases), except for p53 and vascular endothelial growth factor. Our data suggest that protein levels detected by IHC may be a useful complementary tool when mutations are not detected by NGS and also support the idea to expand this approach beyond ADC to include squamous cell carcinoma and even large cell carcinoma, particularly for patients with unusual clinical characteristics. Conversely, well-pronounced immunogenotypic features seemed to predict the clinical outcome after univariate and multivariate analyses. Patients with a solid ADC subtype and mutated genes *EGFR*, *CTLA4*, *PDCD1LG2*, or *ZEB1* complemented with PD-L1 or p53 protein lower expression that only underwent surgical treatment who develop brain metastases may have the worst prognosis.

1. Introduction

Before the 2004 World Health Organization classification, there were no therapeutic implications of distinguishing histologic subtypes such as adenocarcinoma (ADC), squamous cell carcinoma (SqCC), and large cell carcinoma (LCC). Therefore, tumors other than small cell carcinoma were simply lumped together by some pathologists as non–small cell lung carcinomas (NSCLCs), disregarding more specific histologic subtyping. Since then, a surgical intervention has remained the gold standard of treatment for approximately 30% of these patients who presented with resectable stage I, II, or III disease [1], whereas surgical treatment sufficiently early for carcinoma combined with adjuvant chemotherapy in specific cases might improve the long-term outcome [2]. However, almost half of all patients with a diagnosis of NSCLC present with distant metastases [2], and one-third of this patient group will also have brain metastases [2]. Therefore, it is important to analyze predictive factors of survival in patients who received chemotherapy for NSCLC with local and or distant metastases.

The discovery of activating mutations in *EGFR* represents the primary and greatest stage for molecularly guided precision therapy of lung cancer [3]. *EGFR* mutations are frequently observed in females, nonsmokers, and patients with ADC but are rare in patients with SqCC [4]. LCC shares many features with solid ADC [5]; 40% of LCC and solid ADC cases harbor mutations in *KRAS*; EGFR and ALK alterations are rare in this tumor type [5]. So far, all clinical efforts to target KRAS have been unsatisfactory (*KRAS* mutation is also the most frequent driver mutation and is present in 25% of ADCs [6]). *BRAF* mutations have been identified in 2% of patients with NSCLC, half of whom have the BRAF V600E mutation [7]. Additional molecular targets of clinical interest include *ERBB2* amplification [8] and inactivation of tumor suppressor genes (eg, *TP53* [*p53*] and phosphatase and tensin homolog [*PTEN*]) [9]. Immunotherapies targeting programmed cell death 1 (PD-1) and/or PD-1 ligand 1 (PD-L1) may also become important therapeutic modalities in this patient group [10].

In 2017, Reck and Rabe [11] proposed an algorithm for precision diagnosis and treatment of NSCLC, including the morphologic classification of NSCLC based on histopathologic (hematoxylin and eosin) evaluation, molecular analysis for the key treatable oncogenic alterations (EGFR and BRAF V600E mutations and ALK translocations), and additional molecular analyses for selected patients. They also included the assessment of PD-L1 expression by means of immunohistochemical staining. Moreover, chemotherapy remains the first-line treatment for patients with wild-type results of molecular tests [11] (see Supplementary Table S1).

More recently, large-scale molecular profiling of patients with an advanced stage of NSCLC by next-generation sequencing (NGS), led by the Lung Cancer Mutation Consortium, identified multiple cancer driver mutations as potential therapeutic targets [12]. Thus, proper testing methods for treatable oncogenic changes have been used in the routine diagnostic evaluation of patients with an advanced stage of NSCLC [13]. However, the investment necessary to implement this technology is noteworthy. In contrast, immunohistochemistry (IHC) for analysis of protein expression is relatively inexpensive and already an established component of the surgical pathologist's diagnostic armamentarium. Indeed, protein levels detected by IHC can reflect aberrant pathway activation or inactivation and generate functional information on genetic alterations underlying these aberrations [14]. It is therefore a powerful tool complementary to genomic analyses, particularly for those that uncover alterations of unclear significance for tumorigenesis; this procedure is one of the major tasks for interpreting NGS data.

To demonstrate the usefulness of complementary NGS and IHC automated counting, in our cohort, we included only patients without a history of molecularly targeted therapy but who had received chemotherapy for brain metastases. Therefore, we combined NGS technology–based amplicon sequencing with an IHC quantitative panel to maximize the chance of assignment of the enrolled patients to potentially beneficial targeted therapies. We also aimed to determine whether our immunogenotyping approach is useful for the prediction of brain metastases and treatment outcomes.

2. Materials and methods

2.1. Patients

Tumor specimens were obtained from archived formalin-fixed, paraffin-embedded histologic sections from 196 patients with NSCLC at the Clinicas Hospital of University of São Paulo Medical School, Heart Institute, and São Paulo Cancer Institute who underwent surgical resection from January 1, 1995, to December 31, 2014, and received adjuvant chemotherapy. The patients' demographic data and clinical characteristics were retrieved from medical records; they included age, sex, smoking history, tumor size, tumor stage (according to the International Association for the Study of Lung Cancer classification system) [15], and follow-up information for overall survival (OS) rates. Internal ethics committees of the participating institutions approved the study protocol and waived the requirement for informed consent because of the retrospective nature of the study.

2.2. Histopathologic analysis and immunophenotypic classification

Patients' formalin-fixed, paraffin-embedded blocks and archived tissue samples within our Institutional Biobank were studied. Cases were reviewed by expert lung pathologists (E. R. P. and V. L. C.) and thus classified and immunophenotyped according to the 2015 World Health Organization classification of lung tumors [16] into 3 subtypes: ADC (n = 95), SqCC (n = 84), and LCC (n = 17). Tissue sections of poorly differentiated tumors were immunophenotyped by means of TTF1, napsin A, p63, CK5/6, and CK7. In particular, ADC samples were stratified according to the most representative morphologic patterns into lepidic, acinar, papillary, and solid; SqCC into keratinizing and nonkeratinizing; and LCC into tumors with null and unclear immunohistochemical features when positive for CK7 cytokeratin and negative or unclear immunoprofiles and negative for mucin [16].

2.3. Genomic analysis

Genomic DNA was extracted from flash-frozen lung cancer tissue (n = 70) when available in the same patient group (ADCs, 33; SqCCs, 24; LCCs, 13) at the Department of Pathology and Legal Medicine, Ribeirão Preto School of Medicine, University of São Paulo, Ribeirão Preto Facility. Extraction was performed using the QIAamp DNA Mini Kit (Qiagen, Valencia, CA). The quantity and quality of DNA samples were evaluated on a Qubit fluorometer (Life Technologies, Santa Clara, California) and Bioanalyzer (Agilent, Santa Clara, California). Library preparation with the TruSeq Custom Amplicon v1.5 protocol was performed before sequencing on the MiSeq platform (Illumina, San Diego, CA).

Table 1 Clinical characteristics of patients with non–small cell carcinomas

Characteristic	Category	ADC (n = 95)				SqCC (n = 84)		LCC (n = 17)	
		Acinar (n = 38)	Papillary (n = 13)	Lepidic (n = 15)	Solid (n = 29)	Keratinizing (n = 51)	Nonkeratinizing (n = 33)	Null (n = 10)	Unclear (n = 7)
Age (y)	Median	61	65	56	65	69	67	75	70
Sex, n (%)	Female	14 (15)	7 (7)	11 (11)	15 (15)	21 (25)	18 (21)	6 (35)	4 (23)
	Male	24 (25)	6 (6)	4 (4)	14 (15)	30 (36)	15 (18)	4 (23)	3 (17)
Tobacco history [a], n (%)	No	5 (13)	2 (15)	4 (26)	4 (14)	1 (2)	0 (0)	0 (0)	0 (0)
	Yes	21 (55)	7 (54)	7 (46)	13 (45)	25 (49)	10 (30)	2 (20)	2 (29)
Tumor size (cm)	Median	4.5	3.8	3.7	4.5	4.3	3.8	4.5	4.0
Tumor status [b], n (%)	T1	15 (16)	2 (2)	7 (7)	5 (5)	14 (16)	14 (16)	1 (6)	2 (12)
	T2	15 (16)	9 (9)	7 (7)	16 (17)	30 (35)	12 (14)	9 (53)	5 (29)
	T3	8 (8)	1 (1)	1 (1)	6 (6)	5 (6)	7 (8)	0 (0)	0 (0)
	T4	0 (0)	1 (1)	0 (0)	2 (2)	2 (2)	0 (0)	0 (0)	0 (0)
Nodal status [b], n (%)	N0	30 (31)	10 (10)	14 (15)	26 (27)	41 (49)	26 (31)	5 (29)	5 (29)
	N1	8 (8)	3 (3)	1 (1)	3 (23)	10 (12)	7 (8)	5 (29)	2 (12)
IASLC stage [b], n (%)	I	28 (29)	8 (8)	7 (7)	8 (8)	32 (38)	22 (26)	6 (35)	4 (23)
	II	6 (6)	3 (3)	4 (4)	16 (19)	14 (16)	9 (11)	3 (17)	2 (12)
	IIIA	4 (4)	2 (2)	4 (4)	5 (6)	5 (6)	2 (2)	1 (6)	1 (6)
Metastases, n (%)	Brain	1 (1)	2 (2)	2 (2)	2 (2)	1 (1)	0 (0)	1 (6)	0 (0)
Treatment, n (%)	S	38 (40)	13 (13)	15 (16)	29 (30)	51 (61)	33 (39)	10 (59)	7 (41)
	S + C	3 (3)	1 (1)	2 (2)	3 (3)	5 (6)	5 (6)	1 (6)	0 (0)
OS (mo)	Median	29	49	46	23	10	5	40	41

Abbreviations: S, surgery, S + Q, surgery + chemotherapy.

[a] Tobacco history unknown: 32 ADCs (12 acinar, 4 papillary, 4 lepidic, 12 solid), 48 SqCCs (25 keratinizing, 23 nonkeratinizing), 8 LCCs (5 null; 3 unclear).

[b] Per International Association for the Study of Lung Cancer criteria [15].

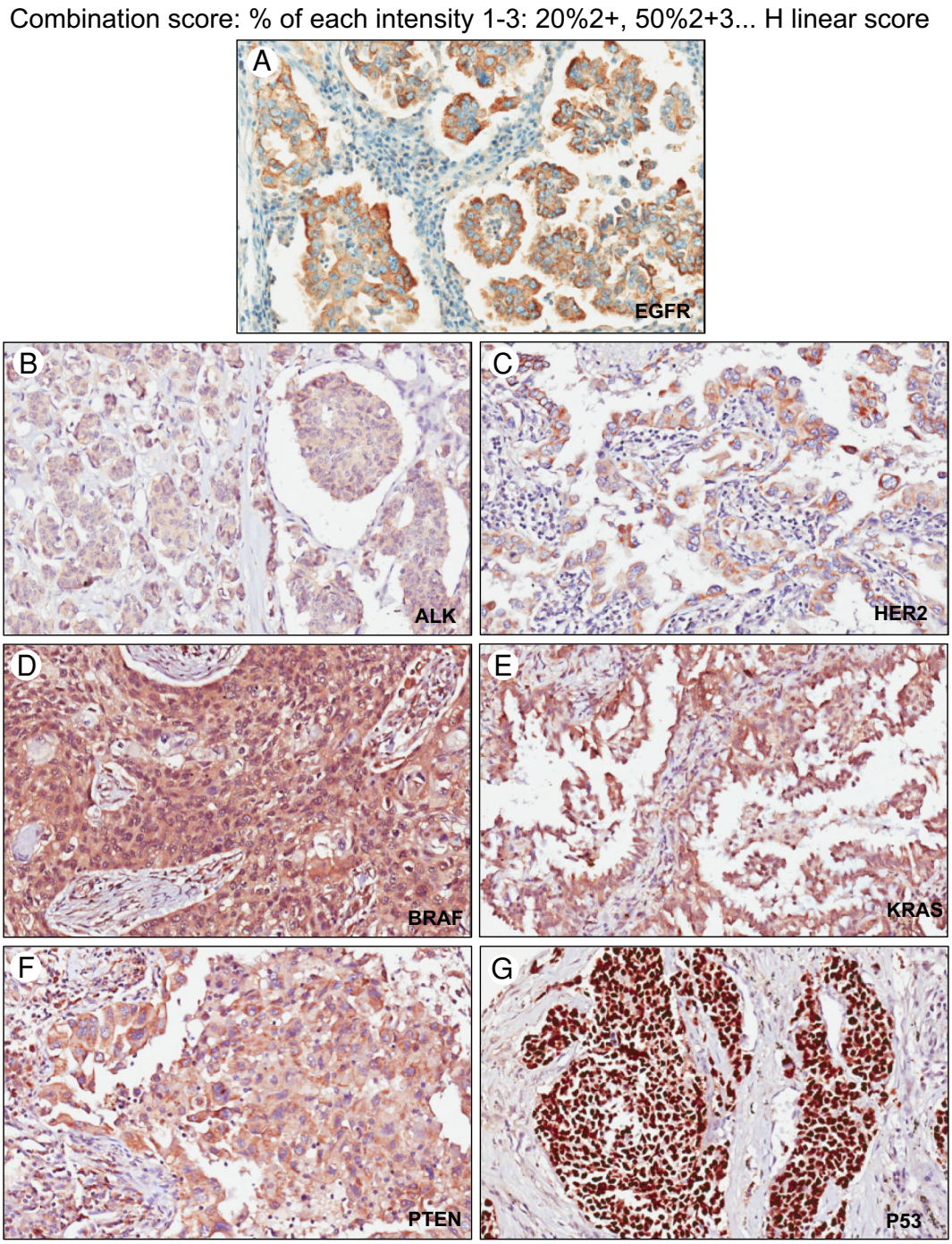

Fig. 1 Protein immunohistochemical staining of NSCLC samples. A-C and E, ADC with positive membranous EGFR, ALK, Her2, or KRAS staining. D, LCC with positive cytoplasmic and membranous BRAF staining. F, Positive membranous and cytoplasmic PTEN staining in SqCC. G, Positive nuclear p53 staining in LCC. A-G, Original magnification ×200.

Sequencing data analysis MiSeq Reporter software (version 2.5.1.3; Illumina) was used to obtain the quality score. We evaluated 24 genes, 102 targets, and 263 amplicons by direct sequencing and verified them by DNA sequencing analysis (Supplementary Table S2). The genes examined were grouped according to their function into oncogenes (*PIK3CA* and *RAB25)*, proto-oncogenes (*BRAF* and *KRAS*), tumor suppressors (*PTEN* and *p53*), immune checkpoints (*CD276*, *CTLA-4*, *PD-L1*, *PD-L2*, *LAGE*, and *VTCNI*), epithelial-mesenchymal transition (EMT) factors, ErbB family members, and vascular endothelial growth factors (VEGFs). For detection of ALK fusions, primers were designed to amplify all known

Table 2 Correlation between histologic types and H-score for protein level in NSCLC (n = 196)

Protein	ADC, mean (median)				SqCC, Mean (median)		LCC, Mean (median)		*P* [a]
	Acinar (n = 38)	Papillary (n = 13)	Lepidic (n = 15)	Solid (n = 29)	Keratinizing (n = 51)	Nonkeratinizing (n = 33)	Null (n = 10)	Unclear (n = 7)	
PD-L1 (%)	23 (0.63)	6 (0.75)	3 (3)	148 (4) [b]	15 (2)	15 (2)	8.5 (0.83)	8.5 (0.83)	.04
ALK-1 (H-score)	2 (0.7)	1.4 (0.2)	18 (12) [b]	6 (5)	15 (9)	12 (7)	2 (0.6)	0 (0)	.04
BRAF (H-score)	67 (61)	33 (23)	95 (82) [b]	75 (65)	63 (60)	59 (57)	61 (45)	58 (42)	.03
EGFR (H-score)	20 (14)	18 (14)	18 (12)	6 (5) [c]	15 (9)	12 (8)	25 (15)	23 (14)	.05
ERBB2 9H-score)	20 (14)	18 (14)	18 (14)	6 (5) [c]	15 (9)	10 (7)	25 (15)	20 (13)	.05
KRAS (H-score)	67 (68)	34 (28)	32 (31)	63 (72)	60 (50)	55 (49)	56 (56)	50 (49)	.10
PTEN (H-score)	39 (31)	33 (23)	52 (45)	57 (58) [c]	45 (31)	40 (30)	50 (57)	45 (50)	.12
P53 (H-score)	163 (48)	30 (24) [d]	188 (60)	116 (54)	134 (47)	130 (40)	485 (88)	450 (70)	.01
VEGFA (H-score)	77 (71)	85 (88)	62 (74)	88 (85)	70 (70)	63 (65)	88 (74)	81 (70)	.93
RAB25 (H-score)	60 (64)	51 (49)	65 (63)	55 (52)	56 (60)	52 (59)	71 (76)	69 (70)	.49
PIK3CA	88 (74)	102 (104)	77 (83)	138 (145)	96 (94)	90 (90)	57 (53)	48 (47)	.51

NOTE. IHC protein staining was scored using a membrane algorithm (PD-L1, EGFR, ALK, ERBB-2, PTEN, PIK3CA) and a cytoplasmic algorithm (PD-L1, BRAF. KRAS, VEGF, RAB5, PIK3CA). Staining intensity, scored as 0 (no staining), 1+ (weak staining), 2+ (moderate staining), or 3+ (strong staining), was multiplied by the percentage of positive cells (0%-100%) for each intensity for a final H-score of 0 to 300. Because PTEN and P53 expression should be either diffusely lost or aberrantly diffusely, either result was qualified as abnormal/"positive" and would be expected to correlate with a mutant event. The average of the number of positive nuclei was expressed as density of cells per millimeter squared. Overexpression was defined as density above or equal median cells per millimeter squared.

[a] Kruskal-Wallis test ($P \leq .05$).

[b] Lepidic ADC significantly increased PD-L1 ($P < .05$), ALK-1 ($P < .05$), and BRAF ($P < .05$) median H-score compared with acinar, papillary and solid.

[c] Predominant solid ADC significantly increased lower H-score for EGFR ($P = .05$) and ERBB2 ($P = .05$), but higher PTEN H-score ($P = .05$).

[d] Papillary ADC significant lower P53 H-score compared with acinar, lepidic, and solid subtypes ($P < .05$).

fusion variants by means of cDNA. All the mutations were verified by analysis of an independent polymerase chain reaction amplicon. For each tissue sample available, the percentage of tumor tissue was assessed beforehand by histologic examination, and the presence of at least 30% of malignant cells was considered adequate for analysis.

2.4. Statistical analysis

The χ^2 test or Fisher exact test was conducted to examine differences in the categorical variables, and the Wilcoxon rank sum test and Kruskal-Wallis test were carried out to detect differences in continuous variables between the patient groups. The OS distributions for the patients were estimated using the Kaplan-Meier method. OS was defined as the interval from surgery to death or last contact. A log-rank test was performed to determine a difference in survival between the groups. Regression analysis of the OS data was performed using the Cox proportional hazards model. The statistical software IBM SPSS (version 22; Armonk, NY) and S-Plus (version 8.04; TIBCO, Palo Alto, CA) were used to perform the computations for all the analyses. Differences were considered statistically significant at $P \leq .05$.

3. Results

Demographic data and clinical characteristics of the patients are shown in Table 1.

3.1. Immunostained protein levels and clinical features

Fig. 1 illustrates representative images of immunostained protein expression.

Table 2 presents the correlation between histologic types and H-scores of protein levels in NSCLC. Protein staining was positive (H-score more than the median value) for PD-L1 in 27% of the samples; ALK, 5%; BRAF, in 5%; EGFR, 20%, ERBB-2, 6%; KRAS, 5%; PTEN, 49%; p53, 48%; VEGF, 90%; and RAB25, 66% of the samples.

TMA tumor sections were obtained from 95 ADCs (38 acinar, 13 papillary, 15 lepidic, and 29 solid tumors), 84 SqCCs (51 keratinizing and 33 nonkeratinizing tumors), and 17 LCCs (10 null and 7 unclear tumor histosubtypes). PD-L1 protein H-score was higher in solid ADCs as compared with acinar, papillary, and lepidic ADCs ($P < .05$). Increased ALK-1 ($P < .05$) and BRAF ($P < .05$) protein positive H-scores were more strongly associated with the lepidic tumor histosubtype as compared with acinar, papillary, and solid ADCs ($P < .05$). In contrast, lower p53 H-scores were more strongly associated with papillary ADCs than with acinar, lepidic, or solid ADCs ($P < .05$). EGFR and ERBB2 protein H-scores were lower in predominantly solid ADCs as compared with the other tumor histosubtypes ($P < .05$ and $P < .05$, respectively). No statistically significant association was detected between all the protein H-scores analyzed and acinar ADCs. Likewise, no significant correlations were detected between ADC histosubtypes and KRAS, VEGFA, RAB25, and PIK3CA protein H-scores. A similar protein H-score median was found for keratinizing and nonkeratinizing SqCCs, as

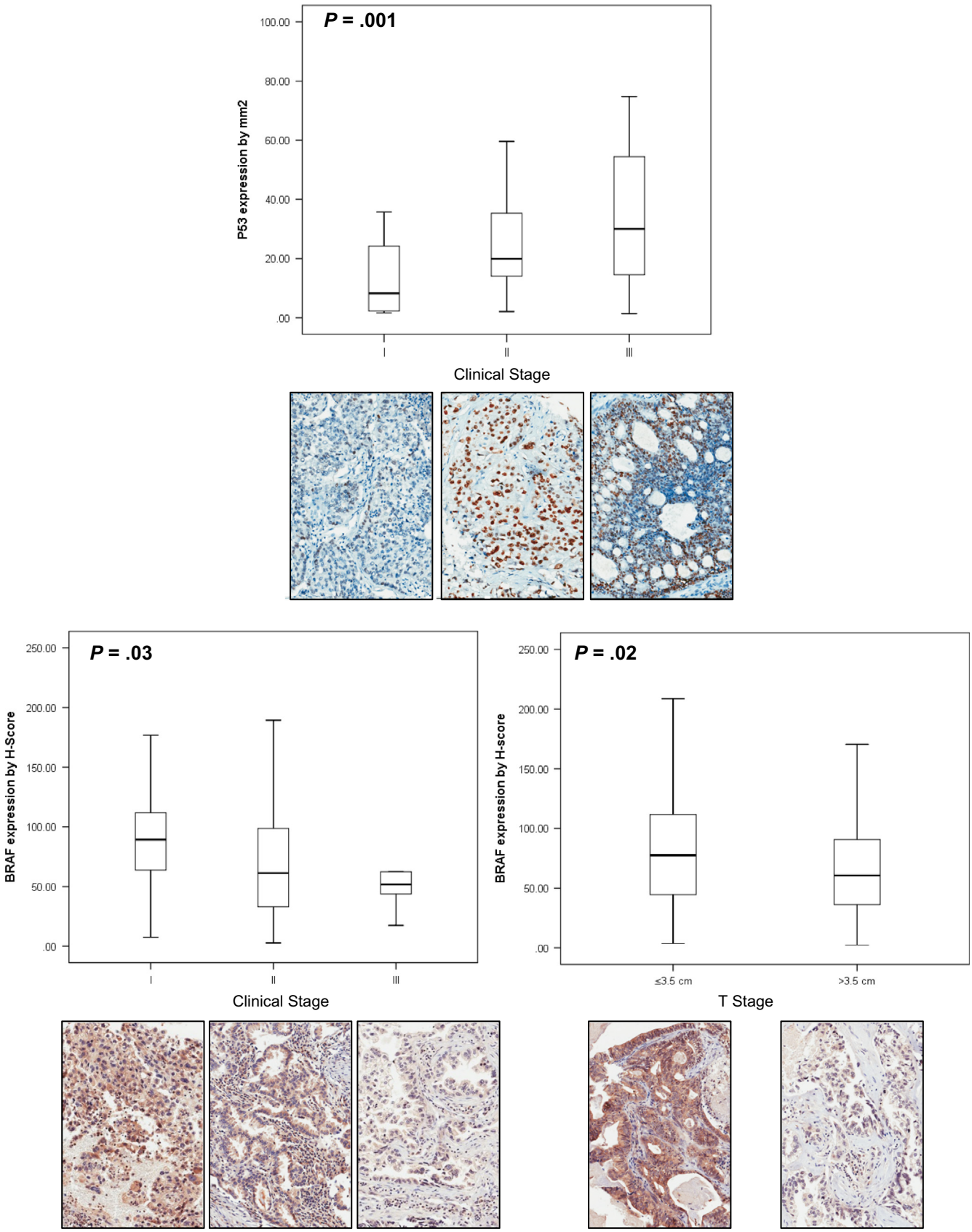

Fig. 2 A distribution box plot of p53 and BRAF intensity of immunostaining by clinical stage (I, II, and III) and T stage (TNM) in NSCLC.

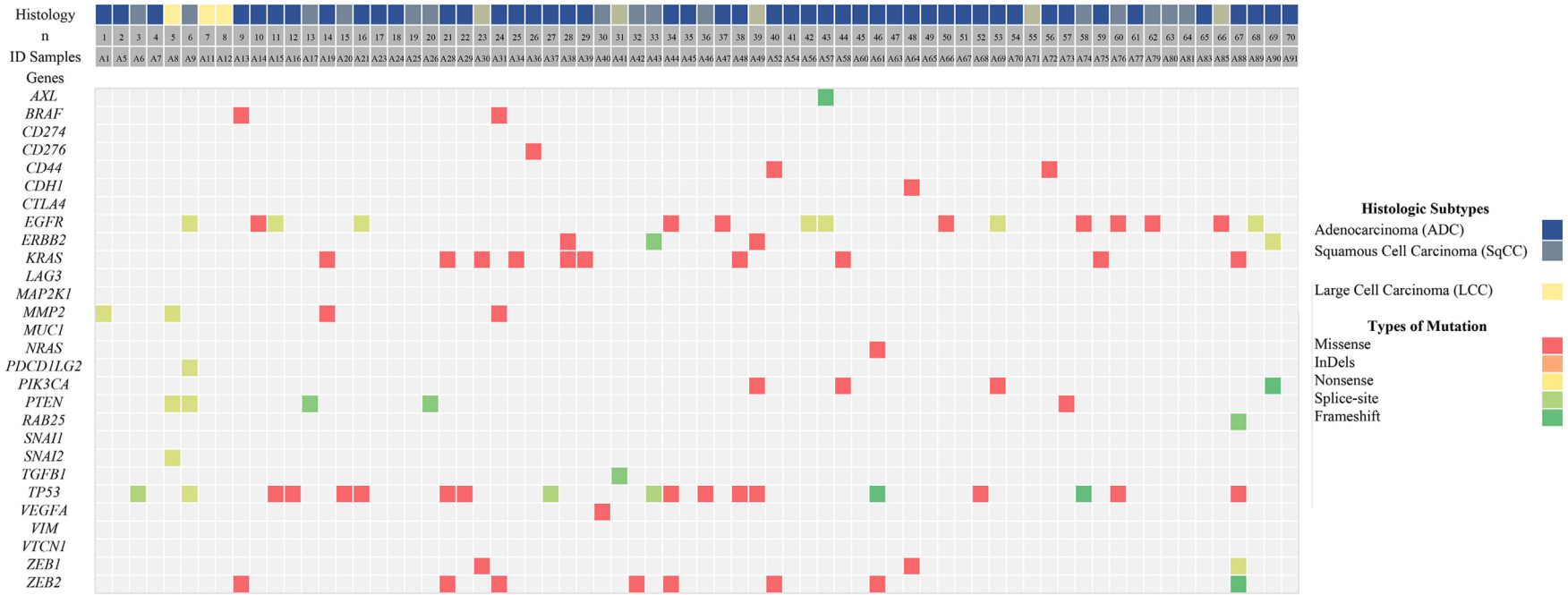

Fig. 3 Profiling of mutations. Gene mutation profiling of NSCLCs. The figure presents gene mutations in each sample. The vertical line shows the name of the mutated genes, and the horizontal line shows the sample number. The mutations in this figure include representative somatic mutations in tumors, tumor suppressor gene mutations, and high-frequency mutations observed in this study. Detected mutations are represented by boxes colored according to the gene mutation.

Table 3 Genes mutations found in 70 primary NSCLC according to histotypes

	ADC (n = 33), n (%)				SqCC (n = 24), n (%)		LCC (n = 13), n (%)		P [a]
	Acinar	Papillary	Lepidic	Solid	Keratinizing	Nonkeratinizing	Null	Unclear	
AXL	12 (36)	5 (15)	4 (12)	12 (36)	18 (75) [b]	6 (25)	8 (61)	5 (29)	.05
BRAF	2 (6)	2 (6)	0 (0)	0 (0)	0 (0)	0 (0)	0 (0)	0 (0)	.76
CD276	3 (9)	2 (6)	1 (3)	5 (21)	2 (8)	1 (4)	3 (31)	0 (0)	.45
CD44	14 (42)	5 (15)	2 (6)	10 (30)	20 (83) [b]	4 (16)	6 (46)	5 (38)	.05
CDH1	1 (3)	0 (0)	0 (0)	0 (0)	0 (0)	0 (0)	0 (0)	0 (0)	.72
CTLA-4	1 (3)	3 (9)	0 (0)	2 (6)	3 (12)	3 (12)	1 (7)	1 (7)	.25
EGFR	3 (9)	0 (0)	1 (3)	6 (18) [c]	4 (16)	3 (12)	2 (15)	2 (15)	.05
ERBB2	2 (6)	0 (0)	0 (0)	0 (0)	1 (4)	1 (4)	1 (5)	0 (0)	.74
KRAS	8 (24) [d]	2 (6)	0 (0)	5 (15)	6 (25)	3 (12)	3 (23)	5 (38)	.03
LAG3	1 (3)	0 (0)	0 (0)	0 (0)	0 (0)	0 (0)	0 (0)	0 (0)	.83
MAP2KI	0 (0)	0 (0)	0 (0)	0 (0)	0 (0)	0 (0)	1 (7)	0 (0)	.70
MMP-2	0 (0)	1 (3)	0 (0)	0 (0)	1 (4)	1 (4)	0 (0)	0 (0)	.47
MUC1	0 (0)	0 (0)	0 (0)	1 (3)	0 (0)	0 (0)	0 (0)	0 (0)	.79
NRAS	0 (0)	0 (0)	0 (0)	1 (3)	0 (0)	0 (0)	0 (0)	0 (0)	.76
PDCD1LG2	12 (36)	4 (12)	2 (6)	13 (40)	18 (75) [b]	4 (16)	6 (46)	5 (38)	.04
PIK3CA	2 (6)	0 (0)	2 (6)	2 (6)	10 (41) [b]	8 (33)	4 (31)	4 (31)	.05
RAB25	1 (3)	0 (0)	0 (0)	0 (0)	0 (0)	0 (0)	0 (0)	0 (0)	.76
SNAIL-1	1 (3)	0 (0)	0 (0)	2 (6)	3 (12)	0 (0)	1 (7)	0 (0)	.91
SNAIL-2	0 (0)	0 (0)	0 (0)	0 (0)	0 (0)	0 (0)	1 (7)	0 (0)	.72
TGF-B1	0 (0)	0 (0)	0 (0)	0 (0)	1 (4)	0 (0)	0 (0)	0 (0)	.89
p53	3 (9)	0 (0)	0 (0)	8 (24) [c]	4 (16)	4 (16)	0 (0)	0 (0)	.001
VEGFA	2 (6)	0 (0)	1 (3)	0 (0)	0 (0)	0 (0)	1 (7)	0 (0)	.03
VIM	0 (0)	0 (0)	0 (0)	0 (0)	0 (0)	0 (0)	1 (7)	0 (0)	.87
ZEB1	3 (9)	0 (0)	0 (0)	14 (12) [c]	0 (0)	0 (0)	0 (0)	0 (0)	.05
ZEB2	1 (3)	0 (0)	0 (0)	1 (3)	0 (0)	0 (0)	0 (0)	0 (0)	.55

[a] Kruskal-Wallis test ($P \leq .05$).
[b] *AXL*, *CD44*, *ERBB2*, *PDCD1LG2*, and *PIK3CA* mutation significantly higher in keratinizing SqCC compared with ADC and LCC patterns.
[c] *EGFR*, *p53*, and *ZEB2* mutation significantly higher in solid ADC than in other subtypes.
[d] KRAS mutation in acinar ADC significantly higher than other subtypes.

was the case for LCC histosubtypes. When the 3 histotypes and their subtypes were compared, only LCC showed significant overexpression of p53 (according to the protein H-score) in the tumor ($P = .05$), thereby yielding a higher H-score median value. No other statistically significant associations were found between the remaining proteins analyzed and histologic subtypes.

In lung cancer specimens, different IHC protein H-scores correlated with the clinical stage, T (TNM tumor) staging, N (TNM nodal) staging, and brain metastases. Specimens from patients with clinical stage III of the disease showed overexpression of the p53 protein (median H-score of 37.12) as compared with patients at clinical stage I (median H-score of 15.80) or II (median H-score of 24.64; $P = .01$). Specimens from patients with clinical stage I harbored overexpression of the BRAF protein (median H-score of 8.64) in comparison with specimens from the patients at clinical stage II (median H-score value of 6.13) or III (median H-score value of 5.17; $P = .03$). Patients at a T1 or T2 (TNM tumor) stage revealed overexpression of the BRAF protein in the tumor (median H-score of 7.81) when compared with specimens from the patients at a T3 or T4 (TNM tumor) stage (median H-score of 5.53; $P = .02$). In patients with brain metastases, primary tumors manifested lower expression of the PIK3CA protein (median H-score of 40) than did tumors without brain metastases (median H-score value of 60; $P = .04$). Regarding the treatment, patients treated only with a surgical intervention had lower expression of the p53 and PD-L1 proteins in the tumor (median H-score values of 23.74 and 1.20, respectively) than did the patients treated with surgical resection followed by chemotherapy (median H-score values of 0.79 and 10.7, respectively; $P = .03$).

We also assessed differences in IHC protein levels according to tumor staging, histotypes, and their histosubtypes (Supplementary Figs. S2 and S3). Patients with solid ADC at clinical stage III showed overexpression of the p53 protein in the tumor (median H-score of 40.87) when compared with patients at clinical stage I (median H-score of 8.24) or II (median H-score of 20.81; $P = .01$). In contrast, patients with SqCC of N2 (TNM nodal) status showed overexpression of the ERBB-2 protein in the tumor (median H-score of 0.49) when compared with patients with N1 (TNM nodal) status (median H-score of 0.32; $P = .02$). In addition, SqCC specimens from patients with the N2 status harbored overexpression of p53 (median H-score of 48.16 cells/mm^2) when compared

Table 4 Comparison of protein overexpression and gene mutation

Genes	Proteins overexpression (H-score more than the median value), case no. (%)										
	PD-L1	ALK	BRAF	CD44	EGFR	ERBB2	KRAS	PTEN	P53	VEGF	RAB25
AXL	29 (51)[a]	33 (46)	34 (49)	30 (44)	34 (47)	34 (49)	27 (43)	29 (48)	32 (48)	2 (4)	4 (6)
BRAF	1 (1.8)	2 (2)	2 (4.5)[b]	0 (0)	0 (0)	0 (0)	0 (0)	0 (0)	0 (0)	0 (0)	0 (0)
CD276	6 (11)	12 (17)	9 (13)	10 (15)	10 (14)	10 (14)	8 (13)	5 (7)	5 (7)	23 (32)	23 (37)
CD44	0 (0)	0 (0)	0 (0)	0 (0)	0 (0)	0 (0)	0 (0)	0 (0)	0 (0)	0 (0)	0 (0)
CDH1	2 (2)	0 (0)	1 (1)	0 (0)	0 (0)	1 (1)	1 (1)	1 (1)	1 (1)	36 (51)	30 (48)
CTLA4	20 (36)[a]	17 (31)	25 (36)	0 (0)	24 (33)	22 (32)	25 (40)	20 (32)	21 (31)	29 (41)	0 (0)
EGFR	10 (14)	14 (20)	13 (19)	11 (16)	10 (14)	7 (10)	9 (15)	9 (15)	7 (10)	26 (37)	22 (35)
ERBB2	1 (2)	3 (4)	2 (3)	2 (3)	4 (5)	1 (1)[b]	1 (1)	2 (3)	3 (4)	33 (44)	23 (39)
KRAS	9 (16)	15 (21)	12 (17)	8 (12)	13 (18)	10 (14)	8 (13)[b]	10 (17)	8 (12)	23 (32)	30 (47)
LAGE3	0 (0)	0 (0)	0 (0)	0 (0)	0 (0)	0 (0)	0 (0)	0 (0)	0 (0)	0 (0)	0 (0)
MAP2K	0 (0)	0 (0)	0 (0)	0 (0)	0 (0)	0 (0)	0 (0)	0 (0)	0 (0)	0 (0)	0 (0)
MMP2	2 (4)	2 (3)	1 (2)	1 (1)	2(3)	1 (1)	1 (2)	1 (2)	1 (1)	35 (49)	30 (48)
MUC1	0 (0)	0 (0)	0 (0)	0 (0)	0 (0)	0 (0)	0 (0)	0 (0)	0 (0)	0 (0)	0 (0)
NRAS	0 (0)	1 (1)	0 (0)	0 (0)	0 (0)	0 (0)	0 (0)	0 (0)	0 (0)	0 (0)	0 (0)
PDCD1LG2	2 (4)[b]	2 (4)	2 (3)	3 (4)	3 (4)	4 (6)	2 (3)	4 (6)	2 (3)	0 (0)	0 (0)
PIK3CA	3 (7)	4 (7)	5 (9)	4 (6)	4 (7)	2 (4)	4 (8)	4 (4)	8 (11)	24 (42)	19 (37)
RAB25	1 (2)	1 (1)	0 (0)	0 (0)	0 (0)	0 (0)	0 (0)	0 (0)	0 (0)	0 (0)	0 (0)
SNAI1	0 (0)	0 (0)	32 (47)	29 (42)	4 (5)	4 (6)	29 (47)	24 (40)	28(91)	34 (48)	29 (47)
TGFB1	0 (0)	0 (0)	0 (0)	0 (0)	0 (0)	0 (0)	0 (0)	0 (0)	0 (0)	0 (0)	0 (0)
p53	32 (48)[a]	11 (15)	0 (0)	0 (0)	0 (0)	0 (0)	0 (0)	0 (0)	30 (46)	0 (0)	0 (0)
VEGFA	27 (49)[a]	26 (46)	23 (48)	31 (45)	32 (28)	32 (46)	30 (48)	28 (47)	34 (57)	33 (46)	30 (48)
VIM	27 (49)[a]	26 (48)	33 (48)	33 (45)	3 (4)	34 (49)	29 (47)	28 (46)	32 (48)	35 (49)	29 (47)
VTCN1	0 (0)	0 (0)	0 (0)	0 (0)	0 (0)	0 (0)	0 (0)	0 (0)	0 (0)	0 (0)	0 (0)
ZEB1	2 (4)	1 (1)	2 (3)	1 (1)	0 (0)	34 (49)	30 (48)	28 (48)	33 (49)	36 (57)	30 (48)

[a] High concordance between gene mutation and PD-L1 protein expression.
[b] Low concordance between gene mutation and protein expression.

with SqCC specimens from patients with N1 status (median H-score of 21.78; $P = .04$). Low expression of the PTEN protein was detected in SqCC specimens from patients with N2 status (median H-score of 16.42) as compared with patients with N1 status (median H-score of 41.67; $P = .01$). Furthermore, patients having SqCC with T3 or T4 (TNM tumor) status showed a higher H-score in the tumor on proteins ERBB2 (median, 0.47) and p53 (median, 64.31) than did the patients with T1 or T2 status (ERBB2: median, 0.36; p53: median, 0.25; $P = .01$; Supplementary Fig. S2). Moreover, tumor specimens from patients with solid ADC and LCC at clinical stage I yielded a high BRAF protein H-score (median, 10.75) in IHC analysis when compared with patients at clinical stage II (median, 53.82) and stage III (median, 55.53; $P = .01$; Fig. 2, Supplementary Fig. S3). Of note, patients with LCC at T1 or T2 stage got a higher ERBB2 protein H-score (median, 0.81) than did patients at the T3 or T4 stage (median, 0.40; $P = .03$). No other correlations were observed between the protein levels and clinical features for NSCLC histotypes or SqCC and LCC histosubtypes.

3.2. Gene profiles and clinical features

Fig. 3 presents the NGS sequence variation among the analyzed cancer-related genes. Of the 70 NSCLC cases examined, at least 1 mutation was found in 13 (18%) cases, whereas 25 (34.7%) cases showed tyrosine kinase receptor mutations, 12 (16.6%) revealed proto-oncogene mutations, 11 showed tumor suppressor mutations (26%), 1 involved immune checkpoint mutations (1.4%), 22 showed EMT-related (30.5%) mutations, and 1 case involved VEGFA mutations (1.4%).

Table 3 shows the genetic status of the patients stratified by histologic types and subtypes. The numbers of tumors with *AXL* or *CD44* mutation were significantly higher for keratinizing SqCC relative to other histotypes and their subtypes ($P = .05$). Equally significant was the higher number of cases with *EGFR*, *p53*, or *ZEB1* mutation in solid ADC than in other types and their subtypes ($P = .05$, $P = .001$, and $P = .05$, respectively). In addition, the number of patients with *KRAS* mutation was significantly higher for acinar ADC compared with other histotypes and their subtypes ($P = .03$). Keratinizing SqCC also harbored a *PDCD1LG2* or *PIK3CA* mutation more frequently than did ADC and LCC subtypes ($P = .04$ and $P = .05$, respectively). ERBB2 mutation was found in 6% of acinar ADC cases, 8% of SqCC cases, and 5% of null LCCs, but these differences did not reach statistical significance. No other statistically significant correlations were found between the remaining analyzed genes and histotypes. Patients with N_0 (TNM nodal) status showed the absence of *EGFR*, *KRAS*, and

Table 5 Descriptive prognostic factors in a Cox proportional hazards model

	Univariate [a]			Multivariate [b]		
	HR (95% CI)	χ^2	*P*	HR (95% CI)	χ^2	*P* [c]
Age (y)						
>65	Reference					
<65	0.99 (0.97-1.01)	0.45	.49			
Sex						
Male	Reference					
Female	2.19 (1.37-3.50)	11.53	.001			
Tobacco history						
No	Reference					
Yes	2.55 (1.07-6.05)	5.63	.01			
Tumor size (cm)						
<4.5	Reference					
>4.5	1.22 (0.92-1.60)	1.90	.16			
Lymph node metastases						
N0	Reference					
N1	1.39 (1.05-1.83)	5.09	.02	1.72 (0.33-2.55)		.43
Brain metastases						
No	Reference					
Yes	1.34 (0.11-2.02)	4.06	.04	1.45 (0.11-2.30)		.04
Stage						
I	Reference					
IIIA	1.45 (1.10-1.89)	7.06	.008			
Histotypes						
SqCC	Reference					
ADC	2.51 (1.11-5.67)	22.19	.001			
Acinar	Reference					
Papillary						
Lepidic						
Solid	1.32 (0.99-2.01)	3.99	.04	1.33 (0.29-6.13)		.05
Surgery	Reference					
Surgery + chemotherapy	0.30 (0.26-4.68)	1.19	.05	1.30 (0.36-4.68)		.05
Genes profile						
Wild-type	Reference					
AXL	1.38 (0.83-2.27)	1.53	.21	2.35 (0.16-4.33)		.03
CD276	1.03 (0.75-1.42)	0.04	.83			
CD44	0.89 (0.66-1.20)	0.57	.44			
CH1	0.21 (0.01-4.48)	4.41	.03	1.54 (0.34-4.78)		.04
CTLA4	1.35 (0.89-2.04)	2.13	.04	1.22 (0.78-2.18)		.04
EGFR	1.12 (0.60-2.09)	2.33	.05	1.45 (0.34-2.89)		.04
ERBB-2	1.78 (0.24-2.53)	2.18	.05			
KRAS	0.96 (0.44-2.10)	0.41	.44			
MMP-2	0.95 (0.46-1.97)	0.01	.89	4.34 (0.80-3.37)		.03
PDCL1LG2	1.28 (0.91-1.80)	2.04	.05	5.57 (0.37-7.10)		.03
PIK3CA	1.57 (0.20-1.63)	4.25	.03	2.32 (0.32-4.78)		.04
p53	1.13 (0.38-3.34)	0.05	.82			
SNAIL-1	0.95 (0.19-1,99)	0.09	.75			
VEGF	0.86 (0.31-2.35)	0.06	.93			
VIM	1.04 (0.36-3.04)	0.07	.71	4.32 (0.45-6.69)		.04
ZEB-1	1.57 (0.23-2.41)	2.30	.05			
Proteins H-score						
<Median						
>Median	Reference					
PD-L1	1.99 (0.99-1.00)	2.14	.05	2.37 (1.20-3.84)		.05
ALK-1	1.07 (0.65-1.74)	0.07	.78			
BRAF	1.09 (0.70-1.70)	0.16	.68			

(*continued on next page*)

Table 5 (*continued*)

	Univariate [a]			Multivariate [b]		
	HR (95% CI)	χ^2	*P*	HR (95% CI)	χ^2	*P* [c]
EGFR	1.26 (0.81-1.94)	1.11	.29			
ERBB2	1.04 (0.68-1.60)	0.04	.84			
KRAS	0.95 (0.60-1.48)	0.05	.81			
PTEN	0.91 (0.58-1.45)	0.13	.71			
P53	1.01 (0.99-1.00)	8.50	.07	1.02 (0.99-1.06)		.05
PIK3CA	1.39 (0.88-2.18)	2.05	.15			
VEGFA	1.00 (0.65-1.53)	0.00	.99			
RAB25	0.84 (0.53-1.32)	0.55	.45			

NOTE. Sex (male, 0; female, 1), smoking status (0, history negative for smoking; 1, history positive for smoking), lymph node and brain metastases (0, negative; 1, positive), and histotypes (acinar, 1; papillary, 2; lepidic, 3; solid, 4; SqCC, 5; LCC, 6). Continuous variables: age, staging, PD-L1 expression, and protein expression.

Abbreviations: CI, confidence interval; HR, hazard ratio.

[a] Univariate analysis is carried out without any adjustment.

[b] In addition to clinically relevant variables, multivariate analysis is carried out on statistically significant parameters obtained from the univariate model.

[c] Statistical results with $P \leq 0.05$.

PIK3CA mutations in the tumor as well as the absence of *ALK* and *ERBB2* aberrations. The absence of brain metastases was associated with wild-type sequences of *EGFR* ($P = .05$), *CD267* ($P = .04$), *CTLA-4* ($P = .05$), and *ZEB1* ($P = .03$).

3.3. A comparison of protein expression using IHC and gene profiles from NGS

Table 4 presents the possible correlations between protein overexpression (H-score more than the median value) and gene profiles. In general, the combination of the detection of protein overexpression by IHC and mutation by NGS by means of the minimal panel (PD-L1, BRAF, EGFR, ERBB2, and KRAS) was rare (ie, represented by a very low percentage of concordant cases), except for p53 and VEGF. In addition, no mutations were found in the following genes: *LAGE3*, *MAP2K*, *MUC1*, *NRAS*, *SNAIL1*, *TGFB1*, and *VTCNI*; these findings may support the utility of IHC analysis for eventual clinical trials and combined therapeutic protocols.

PD-L1 overexpression was associated with overexpression of other proteins such as EGFR, BRAF, ERBB2, and KRAS as well as mutated genes (*AXL*, *CTLA4*, *PDCD1LG2*, *p53*, *VEGFA*, and *VIM*) among other aberrations (see Table 4). With regard to EMT genes, a more expanded panel is necessary to test the combination of expression analysis of other proteins and NGS.

3.4. Correlations of a protein level, gene profile, and clinical outcome

Female patients, smokers, and patients with lymph node metastases, brain metastases, stage IIIA, or ADC were at a high risk of death as compared with male patients, nonsmokers, and patients without lymph node metastases, brain metastases, stages I and II, or SqCC. Mutant oncogene driver *EGFR* significantly increased the risk of death among our patients ($P = .05$). The risk of death was likewise significantly higher among patients having mutant immune checkpoint genes (*CTLA4* and *PDCD1LG2)* or EMT genes (*CH1* and *ZEB1)* in the tumor as compared with those with their wild-type counterparts ($P = .03$ and $P = .04$; $P = .05$ and $P = .03$, respectively). In addition, tumors with the overexpression of the PD-L1 and p53 proteins were associated with a significantly higher risk of death ($P = .05$ and $P = .007$, respectively). Conversely, well-pronounced immunogenotypic features seemed to strongly predict the clinical outcome in the univariate analysis and multivariate analysis. Specifically, patients with solid ADC harboring *EGFR*, *CTLA4*, *PDCD1LG2*, or *ZEB1*, complemented with the lower expression of the PD-L1 or p53 proteins, treated only with surgical resection, who developed brain metastases, were likely to have the worst prognosis (Table 5). The Kaplan-Meier curve revealed longer OS among patients who received surgical treatment followed by patients who received chemotherapy and patients without brain metastases, with high PD-L1 expression, or low p53 expression (Fig. 4).

4. Discussion

In the present work, we demonstrated the usefulness of complementary NGS and IHC counting by analyzing a consecutive cohort of 196 patients with NSCLC who underwent surgical resection followed by chemotherapy for brain metastases but without a history of molecularly targeted therapy. The results uncovered an association with NSCLC histotypes and their subtypes, TNM staging, treatment, and outcome. Specifically, we found that patients with solid ADC, if immunogenotyped even at an early stage of the disease, may benefit from adjuvant chemotherapy and eventual molecularly targeted therapy, thus avoiding a relapse due to brain metastases and poor outcomes.

Recently, NGS allowed us to comprehensively profile tumor gene status. However, so far, studies have failed to provide a comprehensive understanding of the profiles of gene alterations uncovered by NGS and changes in biomarkers revealed by quantitative IHC in lung cancer; these data could complement the potential molecularly targeted therapy. Thus, in this study, we validated IHC quantification of proteins using a membrane algorithm and cytoplasmic algorithm in a way previously reported by other authors [17,18]. This approach reveals that the use of quantitative IHC as a complementary tool of genetic analysis shows promise. Of note, we demonstrated that the combination of the detection of protein overexpression by IHC and mutation by NGS was rare (ie, represented by a very low percentage of concordant cases), except for p53 and VEGF. In addition, no mutations were found in the EMT genes (*LAGE3*, *MAP2K*, *MUC1*, *NRAS*, *SNAIL1*, *TGFB1*, and *VTCNI*); these data may support IHC detection for eventual clinical trials and combined therapeutic protocols. Our observations discussed below also support the idea that it may be useful to expand the NGS and IHC H-score testing beyond ADC to include SqCC and even LCC, particularly for patients with unusual clinical characteristics such as rapid course of progression, younger age, and no history of tobacco smoking.

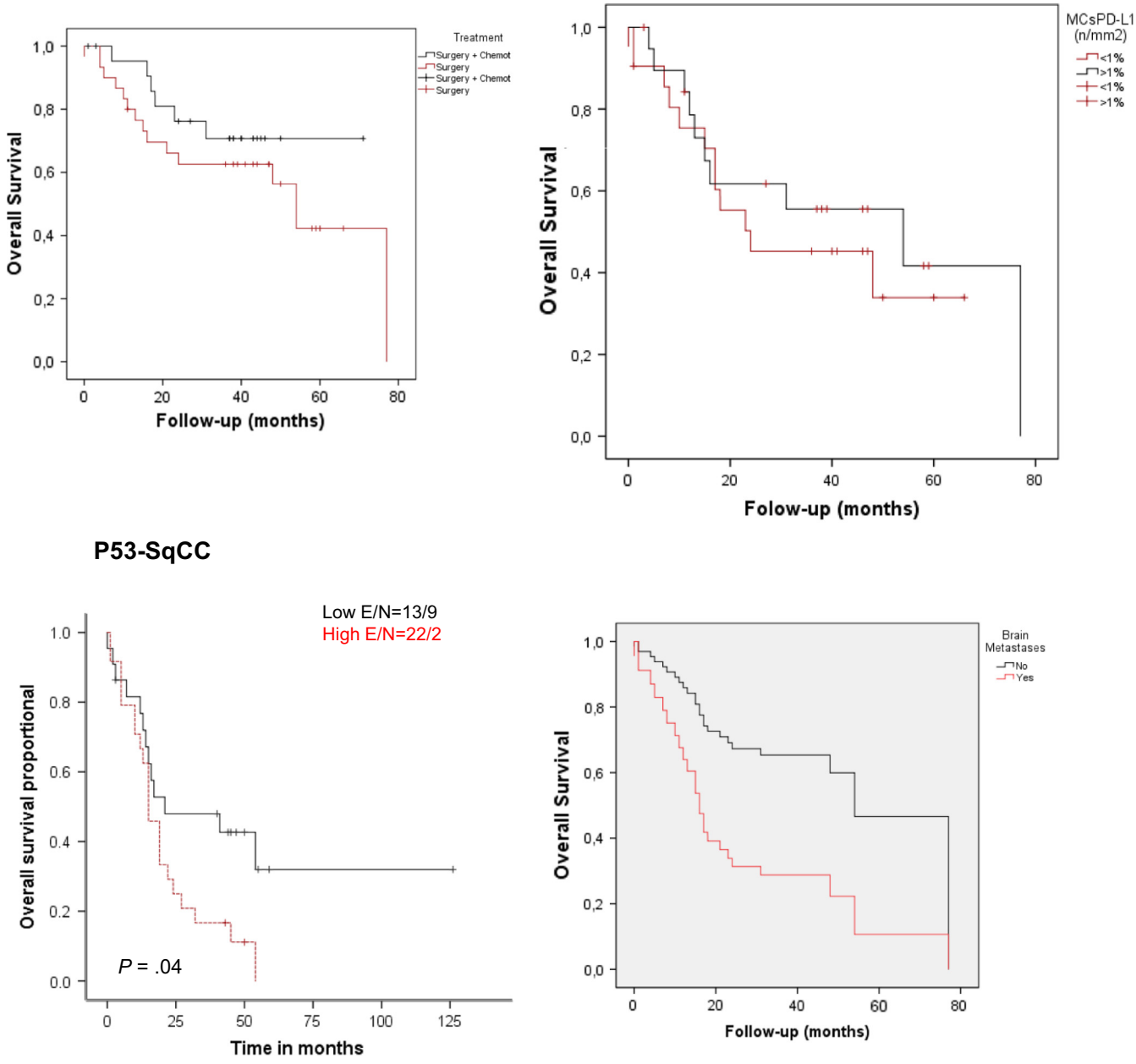

Fig. 4 Kaplan-Meier curves showing that patients with NSCLC and p53 positive staining of 50 cells/mm^2 of greater had significantly lower OS compared with those with p53 of less than 50 cells/mm^2 in univariate analysis (E/N = 25/63 versus 64/10). This prognostic association was also observed in SqCCs (E/N = 13/9 versus 22/2) and ADCs (E/N = 9/39 versus 38/5). E indicates event (death); N, total number.

As previously reported by Huynh et al [18], we found that the PD-L1 protein H-score is higher in a solid ADC subtype compared with acinar, papillary, and lepidic ADCs. Clearly, personalized therapy, including oncological immunotherapy targeting the PD-1–PD-L1 driver pathway and histotypes, has emerged as a promising therapeutic approach to NSCLC [10]. However, the role of these approaches in the treatment of NSCLC has not yet been clarified. In specific subgroups, although patient tumor gene status selection remains important, other factors may also influence PD-L1 expression. For example, PD-L1 expression in malignant cells can be regulated by oncogenic signaling pathways (eg, PTEN loss) with consequent PI3KCA activation [19], thus stimulating cancer cell proliferation. Furthermore, the expression of PD-L1 in lung cancer tissues is heterogeneous because of EMT [20] and ErbB family receptors [8]. In fact, we found that PD-L1 overexpression was also associated with overexpression of other proteins such as EGFR, BRAF, ERBB2, and KRAS, as well as mutated genes (*AXL*, *CTLA4*, *PDCD1LG2*, *p53*, *VEGFA*, and *VIM*), which may influence a therapeutic response to anti–PD-L1 as recently demonstrated by Kim et al [20] and Catacchio et al [21]. We also found that when *CTLA4* is not mutated but overexpressed, as detected by IHC, this finding —when associated with PD-L1—may be important for cancer immunotherapy [21]. Similarly, the VEGF status may yield information on whether patients will respond to bevacizumab combined with atezolizumab and platin-based chemotherapy; this approach was recently proposed as a first-line treatment of metastatic nonsquamous cell NSCLC by Socinski et al [22].

ALK-1 and BRAF proteins are usually expressed by cribriform and solid ADCs, respectively [16], contradicting the results of our study, which revealed that both protein H-scores are most prominent in the lepidic subtype, probably indicating greater accuracy of quantitative IHC for detection of abnormal protein expression. In addition, using an antibody to mutant EGFR, we detected a positive EGFR protein H-score, which was higher than the median score (60%) in 27% of the samples. Positive EGFR protein levels have been identified in 20% to 89% of NSCLC cases, and this large variation may be due to the use of manual cell counting [14]. Thus, our findings are in agreement with the results of many other publications, which have strongly advised against total EGFR staining for selection of patients for EGFR tyrosine kinase inhibitor (TKI) therapy [23]. As expected, we identified high EGFR protein H-scores more frequently in solid ADCs and then in the other histologic types; this finding contradicts the results of studies describing higher frequency of EGFR expression in SqCC compared with lung ADC [24]. Human epidermal growth factor receptor 2 (HER2 or ErbB2) and its protein ERBB2 can be overexpressed, amplified, and/or mutated in malignant tumors and is a candidate for therapeutic targeting. However, molecular and protein associations with a clinical impact of these alterations on lung cancer are controversial [25]. We found that the ERBB2 protein H-score was the highest in solid ADCs compared with other subtypes, again reinforcing the accuracy of the IHC H-score compared with manual cell counting. Comparing the 3 histotypes and their subtypes, we found that only p53 was significantly overexpressed by both subtypes of LCC, thereby yielding a higher H-score median. We uncovered overexpression of the p53 protein in both subtypes of LCC.

In this study, a minimal molecular panel was used [11], along with an expanded molecular panel proposed recently by College of American Pathologists/American Society of Clinical Oncology/International Association for the Study of Lung Cancer (2018). In addition, considering that mutated cancer cells activate immune checkpoints, the mutations of EMT-related and VEGF genes, which are involved in invasion, metastases, and resistance to conventional antineoplastic therapies, were also examined by NGS. We found that the number of tumors with EMT gene mutation related to a tyrosine kinase receptor (*AXL)*, immune checkpoints (*CD44* and *PDCD1LG2)*, or driver oncogene *(PIK3CA)* was higher among keratinizing SqCCs. Notably, increased expression of *AXL* was found by Zhang et al [26] in patients with acquired resistance to EGFR TKI, who identified this EMT gene as a promising therapeutic target whose inhibition may prevent or overcome acquired resistance to EGFR TKI in EGFR-mutant lung cancer patients. Furthermore, high membranous CD44 expression was also identified in lesions (with a mesenchymal phenotype) obtained from lung cancer patients who developed acquired resistance to gefitinib or afatinib [27]. Moreover, upregulation of immunosuppressive gene *PDCD1LG2* and a transcript involved in angiogenesis (VEGFA) and in cell proliferation may prevent the induction of immune-response–related genes after treatment with IFN-γ [28]. Mutation in the *PIK3CA* gene is reported to be frequent in lung SqCC and may confer a survival advantage for the patients. Recently, 7 SqCCs with unusual clinical features were subjected to NGS showing a total of 17 genomic alterations, involving *PIK3CA* in 4 cases, suggesting that this first-line testing is a more comprehensive and effective strategy to design eventual targeted therapy for the patients [29]. In agreement with other reports [29-31], we found that the most commonly mutated genes in solid ADCs were *p53* and *EGFR*, whereas *KRAS* mutation was more frequent in acinar ADC. In addition to these treatment sensitivity mutations in solid ADC, our study revealed targetable mutations in EMT gene *ZEB1*. Epigenetic regulation of the miR-200–ZEB axis is responsible for EMT induction by TGF-β1 in PC9 cells as reported by Zhang et al [32], who demonstrated that decitabine inhibits EMT in NSCLC PC9 cells through its epigenetic therapeutic activity. In agreement with Grob et al [8], *ERBB2* mutation was found in 6% of acinar ADCs, 8% of SqCCs, and 5% of null LCCs, thus prioritizing investigation of HER2-targeting therapy in these tumors.

To validate the usefulness of protein H-scores and gene status in NSCLC specimens, the results were analyzed for possible correlation with staging status, treatment, and outcome. As expected, overexpression of the p53 protein was significantly associated with stage III ADC [33]. In agreement with the results in the study by Kobyakov and colleagues [34], we observed overexpression of the ERBB2 protein in SqCC at

stage T3 or T4 as compared with a T1 or T2 stage tumor. Moreover, in LCC, we observed overexpression of the ERBB2 protein in N1 and T1 tumors. In fact, some reports have described an association between ERBB2 protein expression with ADC and LCC histologic types, indicating similarities between these tumors in terms of advanced and metastatic disease, nodal involvement, and tumor differentiation [35,36]. In SqCC, overexpression of p53 and PTEN proteins was detected in N2 and T3-T4 tumors. Some studies have also revealed that PTEN and p53 tumor suppressor protein levels are more commonly observed in high-grade and advanced-stage SqCC than in ADC cases [37]. Of note, overexpression of p53 and PD-L1 proteins was found in patients treated only with surgical resection as compared with surgery followed by chemotherapy. In addition, tumors with brain metastases express lower levels of the PIK3CA protein than do tumors without brain metastases. Patients at the N_0 stage showed the absence of *EGFR*, *KRAS*, and *PIK3CA* mutations and the absence of *ALK* and *ERBB2* aberrations. The absence of brain metastases was also associated with the wild-type sequences of *EGFR*, *CD267*, *CTLA-4*, and *ZEB1*.

Our study has limitations. To demonstrate the usefulness of IHC level automated counting, our study should have included patients treated with molecularly targeted therapy. However, at our institution, the medication for EGFR-mutated cancers began to be released in 2012, and the test was not performed before that; consequently, we did not have the medication released by the government. Crizotinib, a first-generation anti-ALK fusion agent currently in clinical practice for more than 5 years, was approved in Brazil only in February 2016; the new generation of anti-ALK agents is not yet available in this country. Because the cases involved surgical treatment, at an initial stage, few patients relapsed, and among them, there were SqCC and LCC patients; most ADC patients were not tested, and the tested ones showed wild-type results and therefore did not receive the medication. Approximately 20% of our patients received adjuvant chemotherapy. Despite this scenario on molecular diagnosis for patients within the public health care system, the same does not happen with treatment. Brazil is well known for delaying the approval of new therapeutic options. The last-generation chemotherapeutic agents are available, but targeted therapies are limited.

Besides these limitations, we demonstrated that a combination of NGS and IHC analysis of tumor samples is a feasible method for identification of targetable genomic alterations in patients with NSCLC. In addition, for randomized controlled trials of targeted therapies in the future, identification of specific molecular aberrations was found to be associated with poor survival support a lack of survival-prolonging modalities.

Supplementary data

Supplementary data to this article can be found online at https://doi.org/10.1016/j.humpath.2018.08.026.

Acknowledgment

The authors are grateful to the patients who participated in this study and to Angela Santos for technical assistance.

References

[1] Yoon SM, Shaikh T, Hallman M. Therapeutic management options for stage III non–small cell lung cancer. World J Clin Oncol 2017;8:1-20.
[2] Ahn JS, Ahn YC, Kim JH, et al. Multinational randomized phase III trial with or without consolidation chemotherapy using docetaxel and cisplatin after concurrent chemoradiation in inoperable stage III non–small-cell lung cancer: KCSG-LU05-04. J Clin Oncol 2015;33:2660-6.
[3] Lynch TJ, Bell DW, Sordella R, et al. Activating mutations in the epidermal growth factor receptor underlying responsiveness of non–small-cell lung cancer to gefitinib. N Engl J Med 2004;350:2129-39.
[4] Rosell R, Moran T, Queralt C, et al. Screening for epidermal growth factor receptor mutations in lung cancer. N Engl J Med 2009;361:958-67.
[5] Rossi G, Mengoli MC, Cavazza A, et al. Large cell carcinoma of the lung: clinically oriented classification integrating immunohistochemistry and molecular biology. Virchows Arch 2014;464:61-8.
[6] Suda K, Tomizawa K, Mitsudomi T. Biological and clinical significance of KRAS mutations in lung cancer: an oncogenic driver that contrasts with EGFR mutation. Cancer Metastasis Rev 2010;29:49-60.
[7] Hyman DM, Puzanov I, Subbiah V, et al. Vemurafenib in multiple nonmelanoma cancers with BRAF V600 mutations. N Engl J Med 2015;373:726-36.
[8] Grob TJ, Kannengiesser I, Tsourlakis MC, et al. Heterogeneity of ERBB2 amplification in adenocarcinoma, squamous cell carcinoma and large cell undifferentiated carcinoma of the lung. Mod Pathol 2012;25:1566-73.
[9] Massion PP, Carbone DP. The molecular basis of lung cancer: molecular abnormalities and therapeutic implications. Respir Res 2003;4:12.
[10] Antonia SJ, Villegas A, Daniel D, et al. Durvalumab after chemoradiotherapy in stage III non–small-cell lung cancer. N Engl J Med 2017;377:1919-29.
[11] Reck M, Rabe KF. Precision diagnosis and treatment for advanced non–small-cell lung cancer. N Engl J Med 2017;377:849-61.
[12] Kris MG, Johnson BE, Berry LD, et al. Using multiplexed assays of oncogenic drivers in lung cancers to select targeted drugs. JAMA 2014;311:1998-2006.
[13] Novello S, Barlesi F, Califano R, et al. Metastatic non–small-cell lung cancer: ESMO clinical practice guidelines for diagnosis, treatment and follow-up. Ann Oncol 2016;27(Suppl. 5):v1-v27.
[14] Sholl LM. Protein correlates of molecular alterations in lung adenocarcinoma: immunohistochemistry as a surrogate for molecular analysis. Semin Diagn Pathol 2015;32:325-33.
[15] Travis WD, Brambilla E, Noguchi M, et al. International Association for the Study of Lung Cancer/American Thoracic Society/European Respiratory Society International Multidisciplinary Classification of Lung Adenocarcinoma. J Thorac Oncol 2011;6:244-85.
[16] Travis WD, Brambrilla E, Burke AP, et al. WHO classification of tumours of the lung, pleura, thymus and heart. IARC WHO Classification of Tumours 2015. 4th ed. Geneva: World Health Organization; 2015.
[17] Antonângelo L, Tuma T, Fabro A, et al. Id-1, Id-2, and Id-3 coexpression correlates with prognosis in stage I and II lung adenocarcinoma patients treated with surgery and adjuvant chemotherapy. Exp Biol Med (Maywood) 2016;241:1159-68.
[18] Huynh TG, Morales-Oyarvide V, Campo MJ, et al. Programmed cell death ligand 1 expression in resected lung adenocarcinomas: association with immune microenvironment. J Thorac Oncol 2016;11:1869-78.
[19] Crane CA, Panner A, Murray JC, et al. PI(3) kinase is associated with a mechanism of immunoresistance in breast and prostate cancer. Oncogene 2009;28:306-12.

[20] Kim S, Koh J, Kim MY, et al. PD-L1 expression is associated with epithelial-to-mesenchymal transition in adenocarcinoma of the lung. Hum Pathol 2016;58:7-14.
[21] Catacchio I, Scattone A, Silvestris N, Mangia A. Immune prophets of lung cancer: the prognostic and predictive landscape of cellular and molecular immune markers. Transl Oncol 2018;11:825-35.
[22] Socinski MA, Jotte RM, Cappuzzo F, et al. Atezolizumab for first-line treatment of metastatic nonsquamous NSCLC. N Engl J Med 2018; 378:2288-301.
[23] Cagle PT, Shol LM, Lindeman NI, et al. Template for reporting results of biomarker testing of specimens from patients with non–small cell carcinoma of the lung. Arch Pathol Lab Med 2014;138:171-4.
[24] Zhang Y, Zheng D, Li Y, et al. Comprehensive investigation of clinicopathologic features, oncogenic driver mutations and immunohistochemical markers in peripheral lung squamous cell carcinoma. J Thorac Dis 2017;9:4434-40.
[25] Kim EK, Kim KA, Lee CY, Shim HS. The frequency and clinical impact of HER2 alterations in lung adenocarcinoma. PLoS One 2017;12: e0171280.
[26] Zhang Z, Lee JC, Lin L, et al. Activation of the AXL kinase causes resistance to EGFR-targeted therapy in lung cancer. Nat Genet 2012;44:852-60.
[27] Suda K, Murakami I, Yu H, et al. CD44 facilitates epithelial to mesenchymal transition phenotypic change at acquisition of resistance to EGFR kinase inhibitors in lung cancer. Mol Cancer Ther 2018 [pii: molcanther.1279.2017].
[28] Saigi M, Alburquerque-Bejar JJ, Mc Leer-Florin A, et al. MET-oncogenic and JAK2-inactivating alterations are independent factors that affect regulation of PD-L1 expression in lung cancer. Clin Cancer Res 2018.
[29] Mehrad M, Roy S, Bittar HT, Dacic S. Next-generation sequencing approach to non–small cell lung carcinoma yields more actionable alterations. Arch Pathol Lab Med 2018;142:353-7.
[30] Tsutaa K, Kawagoa M, Inouec E, et al. The utility of the proposed IASLC/ATS/ERS lung adenocarcinoma subtypes for disease prognosis and correlation of driver gene alterations. Lung Cancer 2013;81: 371-6.
[31] Villa C, Cagle PT, Johnson M, et al. Correlation of EGFR mutation status with predominant histologic subtype of adenocarcinoma according to the new lung adenocarcinoma classification of the International Association for the Study of Lung Cancer/American Thoracic Society/European Respiratory Society. Arch Pathol Lab Med 2014;138:1353-7.
[32] Zhang N, Liu Y, Wang Y, Zhao M, Tu L, Luo F. Decitabine reverses TGF-β1–induced epithelial-mesenchymal transition in non–small-cell lung cancer by regulating miR-200/ZEB axis. Drug Des Devel Ther 2017;11:969-83.
[33] Steels E, Paesmans M, Berghmans T, et al. Role of p53 as a prognostic factor for survival in lung cancer: a systematic review of the literature with a meta-analysis. Eur Respir J 2001;18:705-19.
[34] Kobyakov DS, Avdalyan AM, Klimachev VV, Lazarev AF, Lushnikova EL, Nepomnyaschikh LM. Non–small cell lung cancer: HER2 oncogene status. Arkh Patol 2015;77:3-9.
[35] Arcila ME, Chaft JE, Nafa K, et al. Prevalence, clinicopathologic associations, and molecular spectrum of ERBB2 (HER2) tyrosine kinase mutations in lung adenocarcinomas. Clin Cancer Res 2012;18: 4910-8.
[36] Grossi F, Spizzo R, Bordo D, et al. Prognostic stratification of stage IIIA pN2 non–small cell lung cancer by hierarchical clustering analysis of tissue microarray immunostaining data: an Alpe Adria Thoracic Oncology Multidisciplinary Group study (ATOM 014). J Thorac Oncol 2010;5: 1354-60.
[37] Cui M, Augert A, Rongione M, et al. PTEN is a potent suppressor of small cell lung cancer. Mol Cancer Res 2014;12:654-9.